Solid domains in lipid vesicles and scars

Y. Chushak[1,2] and A. Travesset[1,2]

[1] *Physics Department, Iowa State University, Ames, IA, 50011, USA*
[2] *Ames Lab, Ames, IA, 50011, USA*

PACS. 62.20.Dc – Elasticity, elastic constants.
PACS. 61.72.Lk – Linear defects: dislocations, disclinations.
PACS. 87.16.Dg – Membranes, bilayers and vesicles.

Abstract. –
The free energy of a crystalline domain coexisting with a liquid phase on a spherical vesicle may be approximated by an elastic or stretching energy and a line tension term. The stretching energy generally grows as the area of the domain, while the line tension term grows with its perimeter. We show that if the crystalline domain contains defect arrays consisting of finite length grain boundaries of dislocations (scars) the stretching energy grows linearly with a characteristic length of the crystalline domain. We show that this result is critical to understand the existence of solid domains in lipid-bilayers in the strongly segregated two phase region even for small relative area coverages. The domains evolve from caps to stripes that become thinner as the line tension is decreased. We also discuss the implications of the results for other experimental systems and for the general problem that consists in finding the ground state of a very large number of particles constrained to move on a fixed geometry and interacting with an isotropic potential.

Introduction. – Spherical crystals appear in many different contexts. Recent examples include colloids on oil-water interfaces (Colloidosomes) [1], micropatterning of spherical particles [2] relevant for photonic crystals or Clathrin cages, responsible for the vesicular transport of cargo in cells [3] (see [4] for a detailed theoretical study). Crystalline domains covering a fraction of the sphere are also of experimental interest. In the context of lipid rafts [5], confocal fluorescence microscopy studies have revealed the coexistence of fluid and solid domains on giant unilamellar vesicles made of lipid mixtures. The shapes of these solid domains include stripes of different widths and orientations [6–8] as well as spherical caps [9]. Very recently, solid domains in the gel phase, clearly displaying stripes and circular domains have also been investigated by Poon and collaborators [10].

The structure of a crystalline domain on a sphere is just one example of the more general problem of the interplay between crystalline order and geometry, which can be understood from two limiting cases: Crystalline order wins over geometry and the crystal consists of faceted domains with isolated buckling at topological defects [11, 12] (The elastic energy of a faceted icosahedron maybe computed from [12]) or geometry is the victor, and the crystal is able to adapt to a smooth geometry by a proliferation of a well defined array of topological defects (scars) [13]. The intermediate regimes, which are characterized by the ratio of the

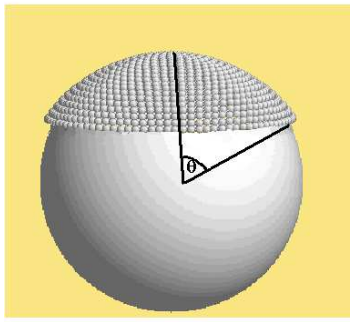

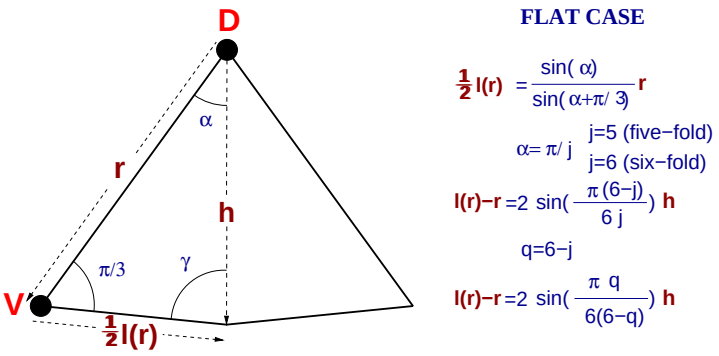

Fig. 1 Fig. 2

Fig. 1 – Definition of the subtended angle θ.

Fig. 2 – Geometrical argument to compute the function $l(r)$ on a plane, which is necessary to obtain the location of the dislocation forming the scars. The same argument can be generalized to any geometry.

bending rigidity to the product of the Young modulus with the radius square of the crystal, are of great interest and have been described in [4, 14]. For solid lipid domains, the faceting scenario has been advocated in [15]. Schneider and Gompper [16], however, have pointed out that the domains observed in [6–8] do not appear consistent with faceted crystalline domains, and have discussed the alternative possibility where crystalline domains remain curved. In that case, the shape of the domains follows from the competition between the stretching energy and the solid-liquid line tension. The free energy is

$$E = E_s + \gamma p \ , \tag{1}$$

where E_s is the stretching or elastic energy, γ the solid-liquid line tension and p the perimeter of the liquid-solid boundary. The analysis in [16] is an expansion that works better for small area coverages. Large domains, which are observed in some experiments [6], pose some problems, as it has been shown that because of the finite gaussian curvature spanned by the curved domains [13], local strains build up, which inevitable lead to the proliferation of topological defects.

In this paper, we show that scars are necessary to understand the shapes and structure of large crystalline domains on spherical vesicles. We determine its structure from general results [17] derived for arbitrary geometries and show that with the inclusion of the scars, the stretching energy is drastically reduced. We believe faceting is unfavorable (to a larger degree, since experimental results do show small shape deformations in some cases [6]) because although the stretching energy of a faceted crystal may only grow logarithmically with its area [11](such as in the case of a buckled conical crystal) it implies a much larger line tension with the coexisting liquid domain. We further assume that the bending rigidity is the same for both solid and liquid domains, which is usually a reasonable approximation. We will be considering a fixed geometry (the sphere) and therefore the bending rigidity will not play a role in determining the shapes and structures of the domains.

Stretching energy of spherical caps. – We first consider the case of an spherical cap on a sphere of radius R, as shown in fig. 1. The elastic stretching energy is

$$E_s = \int d^2\vec{r}(\mu u_{\alpha\beta}^2 + \frac{\lambda}{2}(u_{\alpha\beta})^2), \tag{2}$$

where λ, μ are the Lame coefficients and $u_{\alpha\beta}$ is the strain tensor. Upon minimizing the above expression, the stretching energy of a crystalline domain with radius r_a becomes

$$E_s = K_0 r_a^2 F(\theta) \tag{3}$$

where K_0 is the Young modulus and $\theta = r_a/R$ is half of the total angle subtended by the cap (see fig. 1). The angle θ is related to the relative area covered by the domain

$$\frac{A}{A_0} = \sin^2(\frac{\theta}{2}) \ , \tag{4}$$

where $A_0 = 4\pi R^2$ is the total area of the sphere. The function $F(x)$ in eq. 3 depends on the actual defect distribution within the cap. At small values of x for both a defect free cap or one with a single disclination at its center, the result is [16]

$$F(x) \sim \left\{ \begin{array}{cc} x^4 & \text{no defects} \\ 1 - \frac{3}{2}x^2 & \text{five-fold disclination at the center of the domain} \end{array} \right. \tag{5}$$

for larger values of x the function $F(x)$ might be computed from the results in [13]. We are interested in the regime where θ is not necessarily small, and in that case the stretching energy grows quadratically with the radius of the cap. For reasonable values of the elastic constants and the line tensions, the stretching energy will only allow for small domains ($\theta << 1$).

As already pointed out, in curved geometries the energy maybe reduced by the inclusion of scars. In [17] the precise structure of these scars was determined from analytical arguments. It was shown that the stretching energy of a crystalline domain consisting of a spherical cap, once scars are included, for any value of θ, grows only linearly with the domain radius

$$E_s \sim K_0 a r_a \ , \tag{6}$$

where a is the lattice constant of the crystal. The actual structure of the scars is obtained from the following; First, the cap is divided into j identical triangular wedges of angle $2\alpha = 2\pi/j$, where $j = 5, 6$ depending on whether the center of the cap is a five or six-fold vertex. The disclination charge, defined as $q = 6 - j$ is $q = 1$ for a five-fold and $q = 0$ for a six-fold vertex. The function $l(r)$, which measures the failure to close the wedge with equilateral triangles, is computed from the geometric construction described in fig. 2 for the geometry of interest (in our case the sphere). The location of the dislocations defining the scars is obtained from the equation

$$l(r) - r = na \tag{7}$$

where $n = \pm 1, \pm 2, \pm 3, \cdots$. Additional details, including the explicit form for the function $l(r)$ as well as the proof that such construction leads to a stretching energy with the form of eq. 6 can be found in [17], but it can be more intuitively understood from noticing that the planar result that leads to eq. 6 is a consequence of the triangles on the lattice being very close to equi-lateral. On a general geometry, we can achieve a similar close to equilateral configuration by noticing that Gaussian curvature modifies the area of the wedge at a given radial distance from the center, and therefore, the equi-spacing of dislocations that follows for planar geometries needs to be distorted according to the Gaussian curvature, which is eq. 7. We now show by an explicit numerical minimization that the scars defined by eq. 7 have an energy defined by eq. 6. An example of a typical configuration with scars is shown in fig. 3.

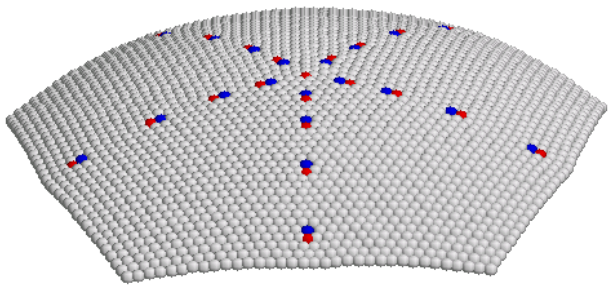

Fig. 3 – Example of a typical scar on a spherical cap. The center of the domain is a five-fold $q = 1$, and 5 grain boundaries each containing four dislocations, with increasing distance within the grain, form the scar. Results are for $\theta = 0.6 \approx 34.4^o$ $(A/A_0 \approx 0.9)$ and $L = 30$.

Numerical Results. – We discretize the elastic energy eq. 2 by considering a discrete triangular lattice with the topology of a disk and open boundary conditions. The discrete stretching energy is

$$E_1(\varepsilon) = \frac{\varepsilon}{2} \sum_{(b,c)} (|\vec{r}_{bc}| - a)^2 \tag{8}$$

where r_{bc} is the nearest-neighbor distance. The coupling ε is related to the Lame coefficients according to $\mu = \sqrt{3}\varepsilon/4$ and $\lambda = \sqrt{3}\varepsilon/4$ [11]. We now consider the cap as made of L monomers along the radial distance from its center, so that $r_a = La$, we write eq. 3 as

$$E_s = K_0 a^2 L^2 F(\theta) \tag{9}$$

Let us recall the results for the plane [18]. Obviously, a perfect triangular lattice with no defects has the lowest stretching energy (zero, in our case). If, however, a planar disk has a disclination at its center, then the scars consist of grain boundaries with equi-spaced dislocations (whose spacing is calculated in fig. 2) and the energy grows linearly with L, a result that can also be proven analytically [18]. Let us now explore the results at finite curvature. It is practical to consider a fixed aperture angle and consider the stretching energy (in units of $K_0 a^2$) divided by the dimensionless number L, so that if the stretching energy behaves linearly with L (as in eq. 6) it will show up as a constant as a function of L. Results for $\theta = 0.6 \approx 34.4^o (A/A_0 \approx 0.9)$ are shown in fig. 4 (The actual configuration for $L = 30$ is shown in fig. 3). For configurations consisting of either a perfect lattice (defect free), a single disclination with no defects, or a central disclination with the equi-spaced radial grain boundaries that minimize the energy in the planar case, the stretching energy grows with the expected quadratic behavior eq. 3, as clearly evidenced by the linear growth with L in

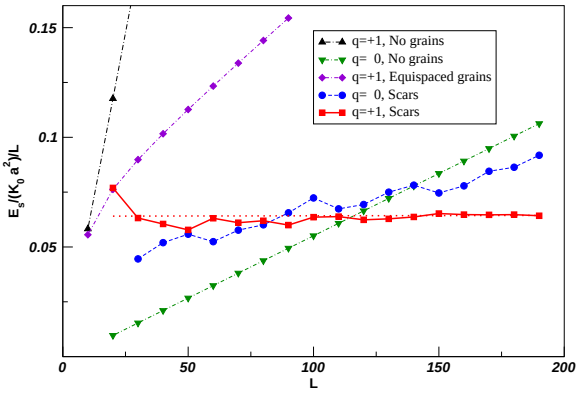

Fig. 4 – Stretching energy in units of $K_0 a^2$ divided by L as a function of the lattice size L. The label $q = 1, 0$ represents whether there is a plus-disclination or a regular vertex at the center of the crystal. Equi-spaced configuration is the configuration that minimizes the plane for $q = +1$. The scars are predicted from eq. 7 as explained in the text. The dotted line is a fit to $q = +1$ scars. Results are for $\theta = 0.6$ ($A/A_0 \approx 0.9$), and $\mu = \lambda = 0.4333$.

the plot. With a five fold at the center and the scars defined by eq. 7, however, the plot of the stretching energy is horizontal, implying that the energy grows linearly with L (eq. 6). The largest system investigated $L = 200$, consists of the order of 10^5 monomers and contains ~ 120 dislocations. If the center of the cap has a six-fold vertex, the stretching energy does show a slight slope. This is due that the theoretical argument eq. 7 places a large number of dislocations close to the boundaries. In other words, the predicted theoretical configuration is very difficult to realize in practice.

Results for aperture angles within the range $\theta = 0.1 \approx 6^o$ ($A/A_0 \approx 3 \cdot 10^{-3}$) to $\theta = 1.0 \approx 60^o$ ($A/A_0 \approx 0.25$) are shown in fig. 5. The numerical results show remarkable agreement with the expected behavior eq. 6. Even for small area fractions ($A/A_0 = 0.05$) a plus disclination and scars are favored, and that for $A/A_0 > 0.04$ the coefficient of the stretching energy eq. 6 is roughly independent of θ. Only for the largest value of θ studied ($\theta = 1$), a slight slope is

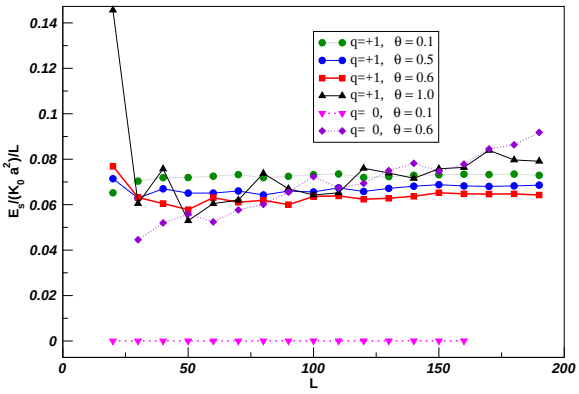

Fig. 5 – Stretching energy in units of $K_0 a^2$ divided by L as a function of the lattice size L for different aperture angles θ and the variable spacing is the energy for the dislocations separation predicted by eq. 7 as explained in the text. Results are for $\mu = \lambda = 0.4333$.

observed in the figure. We believe that this is a consequence that by keeping open boundary conditions, the aperture angle θ is modified from its original value.

There are a few technical aspects that we describe here. The dislocations forming the scars can only be placed at positions defined by lattice points, that is, positions that are integers of the lattice constant. The positions predicted by eq. 7 are in general not integers so the result was rounded, not just to the nearest integer, but to the first odd integer (this choice respects better the structure of the underlying lattice). The defects were placed to the desired positions by using the software developed in [18].

Discussion and Conclusions. – We have shown explicitly that the stretching energy of a spherical cap on a sphere grows linearly with its radius when scars are introduced following eq. 7. A typical scar on a spherical cap is shown in fig. 3. We now consider crystalline domains different than the cap. A ring can be considered as the region defined by two spherical caps of radius r_2, r_1, with $r_2 > r_1$. The width of the ring is d, where $d = r_2 - r_1$. We further assume that the ring is thin $d << r_1$ but not microscopic $d >> a$. The stretching energy of a ring containing scars can be computed as the difference of the stretching energy of the two caps, $E_{st} \sim E_{st}(r_2) - E_{st}(r_1) \sim K_0 a d$ (elastic energy alone tries to avoid Gaussian curvature). Let us now compare the stretching energy of a ring with the stretching energy of a cap, both covering the same area. It is found,

$$E_{st}^{ring} \sim \sqrt{\frac{d}{r_1}} E_{st}^{Cap} \ , \tag{10}$$

since $d/r_1 << 1$, the stretching energy favors rings over caps (both containing scars).

Let us examine now the free energy eq. 1 containing both stretching and line tension energy terms. For a cap of radius r_a and area coverage $A/A_0 > 0.04$, the free energy is

$$E \approx 0.07 K_0 a r_a + 2\pi\gamma r_a \ , \tag{11}$$

where the pre-factor, which we do not claim to be universal as it may depend on the Poisson ratio, is obtained from fig. 5. If

$$\gamma >> \frac{0.07}{2\pi} K_0 a \ , \tag{12}$$

the line tension dominates and a single cap with a disclination at its center and scars will be favored. If the fraction of solid phase is small ($A/A_0 << 0.04$), the cap will consist of a regular vertex and scars. As the line tension is decreased below $0.07 K_0 a/2\pi$, the stretching energy begins to dominate and the system will evolve into rings (or stripes), becoming thinner as the surface tension is decreased. A typical radius for a unilamellar vesicle is $R \sim 30\mu m$. In this case, a domain as small as $1\mu m$ should contain a significant fraction of defects. Typical molecular area of a phospholipid is $\sim 60 \AA^2$ (is actually lower in the crystalline phase). For an aperture angle $\theta = 0.6$ this gives $L \sim 3500$. As it is clear from fig. 5, this value of L is deep into the regime were the stretching energy is linear in L. As a concrete example, in [16] the parameters for a DLPC/DMPC mixture are estimated as $\lambda \approx k_B T/a$, $K_0 \approx 500 k_B T/a^2$. In this case we obtain $0.07 K_0 a/2\pi \approx 5 k_B T/a > k_B T/a \approx \gamma$. That is, the stretching energy dominates and stripes are favored. The effect of gradually adding cholesterol to a DLPC/DHDP mixture amounts to a reduction of the solid-liquid line tension, and as a consequence, the stripes should become thinner. All these observations are in agreement with the experimental results [6].

In this paper, we have ignored the effect of thermal fluctuations on the scars. This problem has been experimentally investigated with colloidosomes in [19], where it has been shown that

dislocations fluctuate (by glide) but on average remain in their equilibrium positions. We expect similar results to apply in general, but the discussion of this point is beyond the scope of this paper.

The results presented in this paper have a broader interest beyond solid domains in lipid mixtures. Our results directly apply to other experimental systems, such as large colloidosomes [1] and the spherical arrays considered in [2]. The numerical evidence summarized by fig. 5 and fig. 4 provide a numerical verification to the theoretical ansatz given in [17] for the ground state of a large number of particles constrained on a given geometry and interacting with an isotropic potential. This is a problem of vibrant activity in the field of potential theory in mathematics, where recent rigorous results have been proved [20]. Our results provide an explicit construction for the ground state, and allows straight-forward generalizations to other geometries. Progress for the torus and negative curvature surfaces will hopefully be reported soon.

* * *

We acknowledge many discussions with Mark Bowick, Doug Hardin, David Nelson, Edward Saff and David Vaknin. AT acknowledges the Benasque center for sciences where some parts of this paper where completed. This work has been supported by NSF grant DMR-0426597, Iowa State Start-up funds and partially supported by DOE under contract No. W-7405-ENG-82.

REFERENCES

[1] Bausch A.R. et al., *Science*, **299** (2003) 1716.
[2] Masuda Y., Itoh T. and Koumoto K., *Adv. Mat.*, **17** (2005) 841.
[3] Alberts et al., *Molecular Biology of the Cell* (Garland Science, New York) 2002, p. 711.
[4] Kohyama T., Kroll D.M. and Gompper G., *Phys. Rev. E*, **68** (2003) 61905.
[5] Simons K. and Vaz W.L.C., *Annu. Rev. Biophys. Biomol. Struct.*, **33** (2004) 269.
[6] Korlach J., Schville P., Webb W.W. and Feigenson G.W., *PNAS*, **96** (1999) 8461.
[7] Feigenson G.W. and Buboltz J.T., *Biophysical J.*, **80** (2001) 2775
[8] Scherfeld D., Kahya N. and Schwille P., *Biophysical J.*, **85** (2003) 3758.
[9] Veatch S.L. and Keller S.L., *Phys. Rev. Lett.*, **94** (2005) 148101.
[10] Gordon V., *Private Communication*, () .
[11] Seung S. and Nelson D.R., *Phys. Rev. A*, **38** (1988) 1005.
[12] Lobkovsky A.E. and Witten T.A., *Phys. Rev. E*, **55** (1997) 1577
[13] Bowick M., Nelson D.R. and Travesset A., *Phys. Rev.B*, **62** (2000) 8738.
[14] Lidmar J., Murny L. and Nelson D.R., *Phys. Rev. E*, **68** (2003) 51910.
[15] Lipowsky R. and Dimova R., *J. Phys. Condes. Matter*, **15S** (2003) 31.
[16] Schneider S. and Gompper G., *Europhys. Lett.*, **70** (2005) 136.
[17] Travesset A., *Phys. Rev. E.*, (2005) , in press.
[18] Travesset A., *Phys. Rev. B*, **68** (2003) 115421.
[19] Lipowsky P. et al., *Nature Materials*, **4** (2005) 407
[20] Hardin D.P. and Saff E.B., *Adv. in Math.*, **193** (2005) 174.